

Computer simulation of an edge dislocation in anthracene crystals

This article has been downloaded from IOPscience. Please scroll down to see the full text article.

1990 J. Phys.: Condens. Matter 2 5489

(<http://iopscience.iop.org/0953-8984/2/25/002>)

View [the table of contents for this issue](#), or go to the [journal homepage](#) for more

Download details:

IP Address: 171.66.16.103

The article was downloaded on 11/05/2010 at 05:59

Please note that [terms and conditions apply](#).

Computer simulation of an edge dislocation in anthracene crystals

N Ide, I Okada and K Kojima

Department of Physics, Yokohama City University, 22-2 Seto, Kanazawa-ku, Yokohama 236, Japan

Received 19 September 1989, in final form 7 February 1990

Abstract. The equilibrium configuration for the core of a [010](001) edge dislocation in an anthracene crystal has been calculated using the atom–atom potential method. A boundary condition has been examined in which molecular rotations were taken into account together with translational displacements on the basis of anisotropic elasticity. The dislocation had a spread-out shear misfit, and the width of the Burgers vector density at half peak height reached 6.2 times the magnitude of the Burgers vector.

1. Introduction

A (001)[010] slip system in anthracene crystals is dominantly operative, but a (001)[110] system is also operative (Robinson and Scott 1967, Kojima and Okada 1989). The elastic energies of [010] dislocations are the lowest of all the possible dislocation energies for a given Burgers vector (Kojima 1979).

The equilibrium configuration for the core of a dislocation in a crystal of aromatic hydrocarbons was first calculated by Mokichev and Pakhomov (1982) for a [010](001) edge dislocation in a naphthalene crystal, using the atom–atom potential method (Silinsh 1980, Pertsin and Kitaigorodsky 1987). The model used consisted of an inner layer of 72 mobile molecules and an outer fixed layer, and was based on isotropic elasticity.

In this paper we will report details of molecular configurations around a [010](001) edge dislocation in an anthracene crystal. We introduced molecular rotations into initial and boundary conditions to a linear approximation, as well as translational displacements, in terms of anisotropic elasticity, because the dimensions of an anthracene molecule are as large as the magnitude of the Burgers vector. A model of size sufficient to study a spread-out misfit in a crystal composed of the large molecules was adopted. Both the methods of static energy minimisation and of molecular dynamics were used to obtain equilibrium configurations. Orientational aspects characteristic of molecular crystals were studied. We were able to perform these time-consuming simulations with the aid of a supercomputer.

2. Method

2.1. Boundary conditions

An anisotropic linear elasticity of the dislocation is used in the initial and boundary conditions. Translational displacements u in terms of anisotropic elasticity can be derived

Table 1. Calculated values of the elastic constants c_{ij} .

c_{ij}	(10^{10} dyn cm $^{-2}$)	c_{ij}	(10^{10} dyn cm $^{-2}$)
c_{11}	12.40	c_{13}	8.40
c_{22}	14.53	c_{15}	1.38
c_{33}	20.13	c_{23}	7.52
c_{44}	2.85	c_{25}	1.90
c_{55}	4.58	c_{35}	-5.03
c_{66}	3.39	c_{46}	1.64
c_{12}	10.42		

from the general equation given by Hirth and Lothe (1982):

$$u_k = \operatorname{Re} \left(- (1/2\pi i) \sum_{n=1}^3 A_k(n) D(n) \ln \eta_n \right) \quad (k = 1, 2 \text{ and } 3) \quad (1)$$

$$\eta_n = x_2 + p_n x_3 \quad (2)$$

where $A_k(n)$, $D(n)$ and p_n are determined from anisotropic elastic constants and the Burgers vector, and the dislocation line runs along the x_1 axis.

For the anthracene crystal with monoclinic symmetry (space group $P2_1/a$, $z = 2$), we have 13 independent elastic constants. To estimate one elastic constant, we have to constitute a few lattices that have appropriate kinds of strains. Since strains are accompanied by molecular rotations, we have to search for orientational parameters corresponding to the minimum energy under the given strains. The lowest possible symmetry (space group P1) is assumed in strained lattices, with two independent molecules in a unit cell. Since the centre of one molecule was located at the lattice point, variation of nine independent parameters (three translational degrees of freedom from the second molecule and six orientational parameters) was considered. A Newton technique was adopted to obtain a strained lattice with a minimum packing energy. The elastic constants are obtained by differentiating these energies numerically with respect to the strains.

The functional form used for the atom-atom potential is the Buckingham function

$$\phi_{ij}(r_{ij}) = -A_{ij}/r_{ij}^6 + B_{ij} \exp(-C_{ij}r_{ij}) \quad (3)$$

where r_{ij} is the distance between non-bonded atoms and A , B and C are empirical parameters presented by Williams (1966) in set IV (Craig and Markey 1979, Dautant and Bonpant 1986, Okada *et al* 1989). The cut-off radius of interaction between atoms was 8 Å throughout this paper. The lattice constants evaluated using this potential were $a_0 = 8.18$ Å, $b_0 = 5.91$ Å, $c_0 = 11.17$ Å, $\beta = 2.16$, $\theta = 1.17$, $\phi = 1.11$ and $\psi = 1.91$, and the packing energy per molecule was 1.02 eV. In lattices with strain ε_{23} or ε_{12} , which break the lattice symmetry $P2_1/a$, the packing energies of the two kinds of molecule are different; one increases, the other decreases and their sum increases.

Table 1 shows the values of the elastic constants c_{ij} evaluated thus. These values are rather larger than the experimental values. The isotropic shear modulus μ_V , averaged following Voigt, is evaluated as 3.55×10^{10} dyn cm $^{-2}$ from our calculated elastic constants, whereas it is evaluated as 3.16×10^{10} dyn cm $^{-2}$ from the experimental values of Danno and Inokuchi (1968), and 3.07×10^{10} dyn cm $^{-2}$ from those of Afanas'eva and Miasnikova (1970). We also used all the other potential parameter sets cited by Pertsin and Kitaigorodsky (1987), but the differences between the calculated and experimental

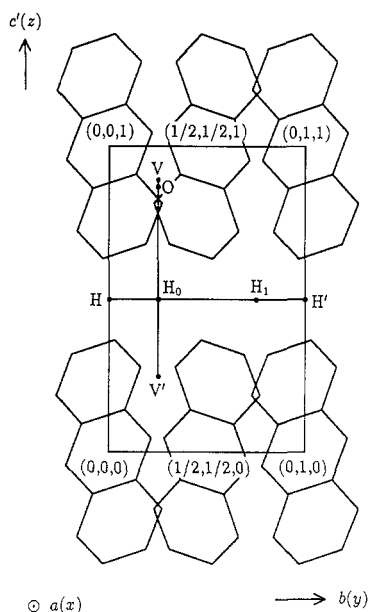


Figure 1. A projection in the bc' plane of a perfect crystal. The influence on the dislocation energy of changing the position of the dislocation in the boundary condition was evaluated on the lines HH' and VV' . The position corresponding to the minimum energy is indicated by O . The (l_1, l_2, l_3) denote lattice sites of molecules.

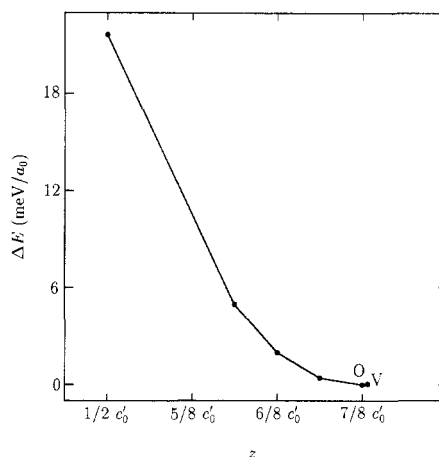


Figure 2. The dislocation energy after relaxation versus the position of the dislocation for the boundary condition. The positions of the dislocation are on the line H_0V in figure 1.

values were of the same order. The changes in Euler angle per unit strain were also calculated. For the strains ϵ_{11} , ϵ_{22} , ϵ_{33} and ϵ_{31} , the relations between the Euler angles (Okada *et al* 1989) of molecules at the corners of a basal unit lattice (1) and those at the centre (2) ($\theta_1 = \pi - \theta_2$, $\phi_1 = -\phi_2$ and $\psi_1 = \pi + \psi_2$) were conserved and the symmetry $P2_1/a$ was retained. For the other strains, ϵ_{23} and ϵ_{12} , the relations between the two kinds of molecule were not conserved.

In addition to translational displacements, we introduce molecular rotations into the initial and boundary conditions to a linear approximation, because the dimensions of an anthracene molecule are as large as the magnitude of the Burgers vector. The strains can be derived from equation (1) and molecular rotations proportional to them are estimated from these strains and the changes in Euler angle per unit strain. Deformations, in general, are accompanied by rigid-body rotations ($\frac{1}{2} \text{rot } \mathbf{u}$) and these also cause molecules to rotate. The magnitudes of these rotations are estimated at the centres of the molecules, and these two kinds of molecular rotation are added.

2.2. Model

Our model for dealing with the relaxation of molecules around the dislocation consists of two layers. One is the outer rigid layer where molecules are held in the positions described above. The other is the inner layer, which consists of the relaxable molecules whose centres lie within a cylinder of radius r_{rel} with its centre at the dislocation line.

Figure 1 shows a projection in the bc' plane of a unit cell of a perfect crystal. The dislocation line runs along the a axis and the slip plane is parallel to the ab plane.

There are two extra molecular half-planes below the slip plane. In the direction of the dislocation, there are two non-equivalent planes, with molecules at the corner sites of the basal unit lattice and at the centre. In the perfect crystal of anthracene, there is a glide symmetry between these two kinds of molecule and the line VV' in the figure is in the glide plane perpendicular to the b axis. To simulate an infinitely long, straight dislocation, periodic boundary conditions are imposed along the dislocation line.

To search for an appropriate position of the dislocation for the initial and boundary conditions, the centre of the dislocation was put at various points along the lines HH' and VV' in the figure. The energies after relaxation were compared for these cases. Among the dislocations with centres on the line HH' , that with its centre at the point H_0 has the lowest energy and that with its centre at the point H_1 has the highest energy. Among dislocations centred on the line VV' , that with its centre at the point O has the lowest dislocation energy and that with its centre at the point V' has the highest. Figure 2 shows the effect of changing the positions of the dislocations for the boundary condition on the energies after relaxation. In this estimation, the positions of the dislocations were on the line H_0V and the value of the relaxation radius r_{rel} was $8b$, where b is the magnitude of the Burgers vector ($=b_0$). The coordinate of the point O corresponding to the minimum energy was $(y, z) = (\frac{1}{4}b_0, \frac{7}{8}c'_0)$, where c'_0 is a unit length of the c' axis.

In order to keep the calculation of the molecular rotations easy, we did not use the boundary-condition technique of making the displacements symmetric with respect to the plane through the centre of an edge dislocation (Cotterill and Doyama 1966); but the symmetry was obtained almost completely after relaxation as we will see later.

2.3. Procedure of simulation

To obtain the equilibrium configuration of molecules in the inner layer, we have tried both the methods of static energy minimisation and of molecular dynamics. In the static minimisation, a method of steepest descent is applied repeatedly until all matrices $\{\partial^2 E_{MR}/\partial x_i \partial x_j\}$ become positive definite and remain so for about ten steps (where E_{MR} denotes the energy of a molecular row parallel to the dislocation line). Then a Newton method is used to make convergence rapid. In the molecular dynamics, the crystal is quenched every time the total kinetic energy reaches a maximum (Gibson *et al* 1960). It was confirmed that the two methods gave the same results as regards the molecular configurations.

The upper limit of the convergence error was estimated to be $4 \text{ meV}/a_0$ for the largest model with $r_{rel} = 16b$ (96 \AA , 1062 molecules in the inner layer). Results of calculations, which will be given later, were obtained by the use of a model of this size.

3. Results

3.1. Equilibrium configurations around the dislocation

Figure 3 shows a projection in the bc' plane of molecular centres after relaxation, and equipotential curves Δu around the dislocation; Δu is the packing energy per unit lattice relative to that of a perfect crystal. It is obvious that the dislocation has a spread-out shear misfit along the slip plane, and that a rectangular region where the energies Δu are almost equal exists around the centre of the dislocation. The plane AA' through the centre of the dislocation is almost a symmetry plane. Curvatures of molecular planes parallel to the slip plane became very small in the core region after the relaxation.

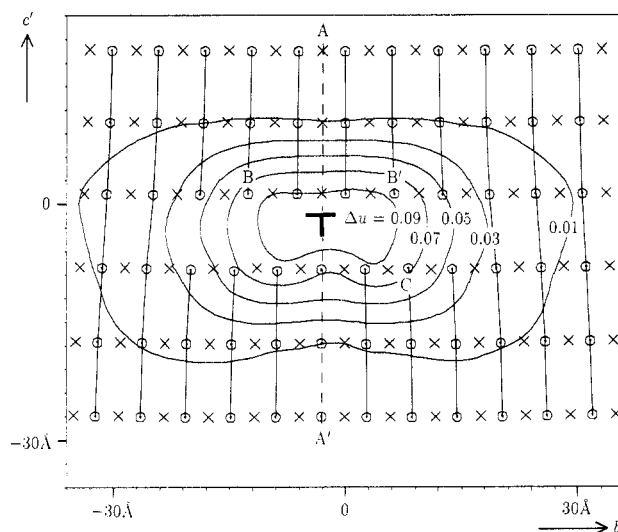


Figure 3. A projection in the bc' plane of molecular centres after relaxation and equipotential curves Δu (in eV). Crosses denote corner molecules and circles denote centre molecules.

Equipotential curves became smooth only if the energies of a corner molecule and a centre molecule were summed, because the effects of the shear strain ϵ_{23} on the two kinds of molecule are different; for example, the energies of the molecules just below the slip plane are 30 meV ($l_2 = -\frac{3}{2}$), 45 (-1), 39 ($-\frac{1}{2}$), 47 (0), 33 ($\frac{1}{2}$), 33 (1), 51 ($\frac{3}{2}$), 39 (2), 40 ($\frac{5}{2}$), 27 (3). The equipotential curves are slightly asymmetric in the core region, as pointed out for a naphthalene crystal by Mokichev and Pakhomov (1982). The high-energy region spreads widely, in contrast to the result for a naphthalene crystal.

The distribution of the strain ϵ_{22} in the direction parallel to the slip plane was also calculated. The value of the strain is small even in the core region since the core spreads widely. Its maximum value is only 7% in the upper half-plane and its minimum value is -5% in the lower half-plane.

Oriental aspects of molecules around the dislocation were investigated in detail. The changes in the Euler angles are larger on the side with the extra half-planes than on the other. The changes in the Euler angles of the centre molecules in the plane just below the slip plane are shown in figure 4(a), and those of the corner molecules are shown in figure 4(b). It is obvious from these diagrams that the changes reach maxima, not at the centre, but at a distance $2b - 3b$ from the centre of the dislocation; $\Delta\theta = 6.5^\circ$, $\Delta\phi = 4.6^\circ$, $\Delta\psi = 10.7^\circ$. These values are about two-thirds of those for a naphthalene crystal calculated by Mokichev and Pakhomov (1982). Curves in (a) and (b) indicate that there is some approximate symmetry between the corner molecules and the centre molecules with respect to the plane AA' . That symmetry is glide-symmetry-like; this may come from the fact that there is a glide symmetry between the two kinds of molecule in the perfect crystal and the shear stress around the dislocation is antisymmetric with respect to the plane AA' . It would be a true glide symmetry if the two kinds of molecule were distributed continuously in each plane.

Figure 5 shows distribution densities of the Burgers vector along the basal slip plane, ρ_y and ρ_x (Viteck *et al* 1971). The density after relaxation deviates substantially from that before relaxation in a wide range from the centre to about $8b$. The core of the

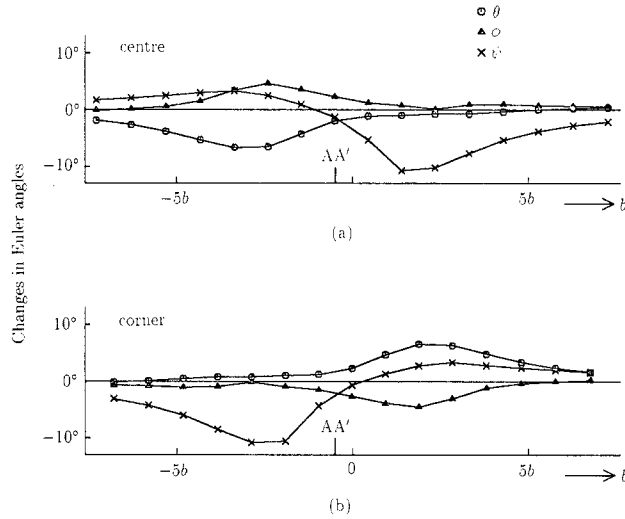


Figure 4. Orientational aspects of molecules around the dislocation. (a) Changes in Euler angles of the centre molecules in the ab plane just below the slip plane; and (b) those of the corner molecules.

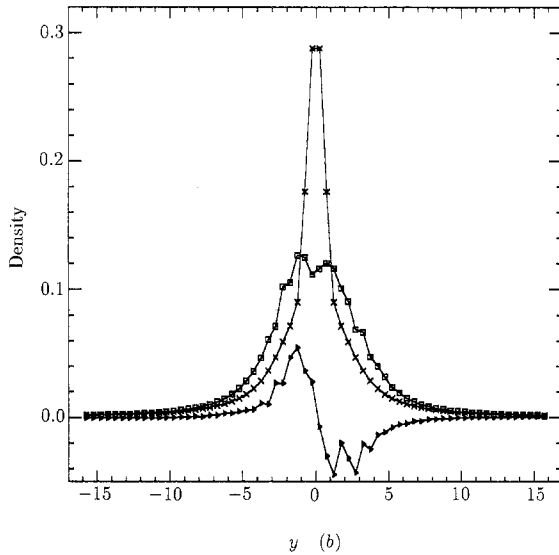


Figure 5. Distribution densities of the Burgers vector along the basal slip plane, ρ_y and ρ_x . Crosses: ρ_y before the relaxation; squares: ρ_y after the relaxation; triangles: ρ_x after the relaxation.

dislocation was not dissociated into two typical partials, but was spread out widely. The width of the core at half peak height is large, being $6.2b$ for the relaxed crystal, in comparison with $2b$ for the unrelaxed crystal. It is seen from ρ_x in the figure that only the molecules close to the centre of the dislocation deviate from the molecular plane, and that this deviation is small.

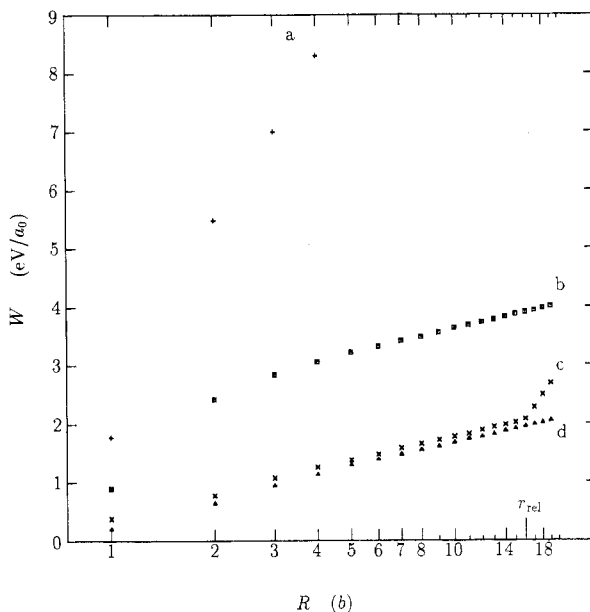


Figure 6. Dislocation energies versus distance from the dislocation line: (a) before relaxation, only translational displacements in elasticity; (b) before relaxation, translational and rotational displacements in elasticity; (c) after relaxation, starting from (a); (d) after relaxation, starting from (b).

3.2. Energy distribution

The strain energy per repeated distance a_0 of an edge dislocation may be written as

$$W = E_d \ln(R/r_0) \quad (4)$$

where E_d is called the pre-logarithmic energy factor, r_0 is called the effective core radius and R is the outer radius of a circular cylinder within which the energy is evaluated. The value of E_d was estimated to be $0.60 \text{ eV}/a_0$ from the anisotropic elastic constants obtained in section 2.1.

The stored energies of the dislocation versus $\ln R$ are shown in figure 6 for four different configurations. To evaluate the influence on the energy of the rotating molecules for the boundary condition, the models with both the translational displacements and rotations, (b) and (d), and with only the translational displacements (a) and (c), were used. The upper plots, (a) and (b), correspond to the configurations before relaxation. These display clearly that the effect of molecular rotations on the energies is very strong. The observed value for the slope of (b) was reduced to a seventh of that of (a) by rotating the molecules in the linear approximation; $E_d(a) = 3.9 \text{ eV}/a_0$, $E_d(b) = 0.60 \text{ eV}/a_0$. The value of $E_d(b)$ agrees very well with that of E_d given above.

The lower plots, (c) and (d), correspond to the configurations after relaxation. The observed values for the slopes of (c) and (d) were $E_d(c) = 0.58 \text{ eV}/a_0$ and $E_d(d) = 0.57 \text{ eV}/a_0$, respectively. These values are slightly smaller than the value of E_d based on the elasticity. This results from the effect of the spread of the core extending far from the core, as figure 5 shows. The plots (c) have a kink at the relaxation radius, because this model has the outer fixed layer, where molecules are held in the same orientations

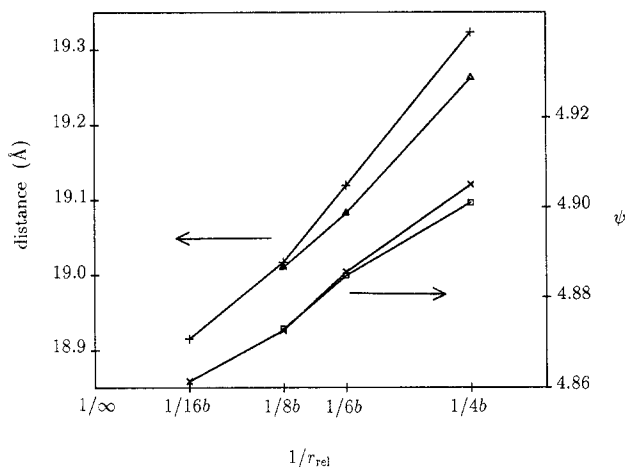


Figure 7. The bond length between the molecules B and B' and the Euler angle ψ of the molecule C as a function of model size. The positions of the molecules B, B' and C are shown in figure 3. The relaxation radii are $4b$ (68 relaxable molecules), $6b$ (144), $8b$ (266) and $16b$ (1062). +, ×: with rotations. Δ, □: without rotations.

as in a perfect crystal. Molecular rotations in the outer fixed layer, however, do not have so strong an effect on the energy of the inner relaxable layer when r_{rel} is as large as $16b$.

The effective core radius r_0 was estimated to be $0.53b$ from figure 6. The core radius cannot be determined accurately from figure 6, but it is about $5b$ judging from figure 5. This yields a core energy of $1.28 \text{ eV}/a_0$, which is 125% of the packing energy per molecule in a perfect crystal.

3.3. Effects of the boundary conditions

To evaluate the effects of the boundary conditions, several runs were made using both types of boundary—with the rotations and without the rotations. In our case, the effects of the rotations and the model size are reflected in changes in length of some intermolecular bonds and in Euler angles of molecules in the core. The two of these that are the most marked are displayed in figure 7 for models of increasing size. Although even for the larger model the bond length and the Euler angle are still varying, differences between the largest model used and an infinitely large model will be of the order of 0.1 \AA (0.5%) in the bond length and 0.01 in the Euler angle ψ . The influence of rotating molecules becomes less important for models with r_{rel} larger than $8b$.

The effects of model size on the Burgers vector density ρ_y were also examined. The complicated variations of ρ_y in the misfit region in figure 5 were barely affected for the model with r_{rel} larger than $6b$. These variations would come mainly from the relationship between neighbouring molecules. Judging from the ρ_y curves for these four models, the model size $r_{rel} = 8b$ is sufficiently accurate for use in a qualitative calculation of the core structure. The effects on ρ_y of the molecular rotation were small in comparison with the size effects.

The energy distribution was affected strongly by the model size. Especially in the smaller models, energies of molecules just near the centre of the dislocation became higher than those of the surrounding molecules.

4. Discussion

It was found that the edge dislocation in an anthracene crystal had a spread-out shear misfit along the slip plane. The distribution density ρ_y of the Burgers vector along the slip plane deviated substantially from that of the elastic solution in the wide range from the centre to a distance $8b$. This seems to be a characteristic feature of aromatic crystals, because strains could not converge into a narrow region due to the large rigid bodies of the molecules. This dislocation had some symmetry, which looked like a glide symmetry.

The influence on the core structure of rotating molecules in the outer rigid layer became less important for a model with a relaxation radius larger than $8b$. The effects of the model size on the intermolecular bond lengths and the Euler angles are not negligible even for the model with the relaxation radius $16b$. However, judging from the distribution density ρ_y of the Burgers vector, the model size with relaxation radius $8b$ is sufficiently accurate for a qualitative calculation of the core structure.

Acknowledgments

We would like to thank Mr I Funahashi and Mr R Iwasaki for valuable help with computations. We also thank the staff of the Computer Centre of Yokohama City University for useful advice. The numerical calculations were partially carried out at the Computer Centre of Tokyo University. This work was supported in part by a Grant-in-Aid for Scientific Research from the Ministry of Education, Science and Culture, Japan.

References

- Afanas'eva G K and Miasnikova R M 1970 *Crystallography* **15** 189
Cotterill R M and Doyama M 1966 *Phys. Rev.* **145** 465
Craig D P and Markey B R 1979 *Chem. Phys. Lett.* **62** 223
Danno T and Inokuchi H 1968 *Bull. Chem. Soc. Japan* **41** 1783
Dautant A and Bonpant L 1986 *Mol. Cryst. Liq. Cryst.* **137** 221
Gibson J B, Goland A N, Milgram M and Vineyard G H 1960 *Phys. Rev.* **120** 1229
Hirth J P and Lothe J 1982 *Theory of Dislocations* (New York: McGraw-Hill) p 436
Kojima K 1979 *Phys. Status Solidi a* **51** 71
Kojima K and Okada I 1989 *Phil. Mag.* in press
Mokichev N N and Pakhomov L G 1982 *Sov. Phys.—Solid State* **24** 1925
Okada I, Sugawara M and Kojima K 1989 *J. Phys.: Condens. Matter* **1** 3555
Pertsin A J and Kitaigorodsky A I 1987 *The Atom—Atom Potential Method* (Berlin: Springer) p 69
Robinson P M and Scott H G 1967 *Acta Metall.* **15** 1581
Silinsh E A 1980 *Organic Molecular Crystals* (Berlin: Springer) p 5
Viteck V, Lejcek L and Bowen D K 1971 *Interatomic Potentials and Simulation of Lattice Defects* ed P Gehlen *et al* (New York: Plenum)
Williams D E 1966 *J. Chem. Phys.* **45** 3770